Molecular Crystals and Liquid Crystals
Publication details, including instructions for authors and subscription information:
http://www.tandfonline.com/loi/gmcl16

On the Mechanism of Shear Induced Texture Changes in Cholesterics-Electric Field Effects

J. M. Pochan [a], P. F. Erhardt [a] & W. C. Richards [a]
[a] Xerox Corporation Rochester Research Center, Webster, New York, 14580

Version of record first published: 21 Mar 2007.

To cite this article: J. M. Pochan , P. F. Erhardt & W. C. Richards (1973): On the Mechanism of Shear Induced Texture Changes in Cholesterics-Electric Field Effects, Molecular Crystals and Liquid Crystals, 24:1-2, 89-102

To link to this article: http://dx.doi.org/10.1080/15421407308083391

Molecular Crystals and Liquid Crystals. 1973. Vol. 24, pp. 89–102

On the Mechanism of Shear Induced Texture Changes in Cholesterics–Electric Field Effects†

J. M. POCHAN, P. F. ERHARDT and W. C. RICHARDS

Xerox Corporation
Rochester Research Center
Webster, New York 14580

Received November 3, 1972; in revised form January 24, 1973

Abstract—Cholesteric systems are being used for display devices because they form several textures each having different optical properties. These textures are: Grandjean (highly reflective); focal conic (highly scattering); and homeotropic (practically transparent). In earlier papers, we have shown that shear induced transitions between these textures can be produced. These transitions are accompanied by color changes in the Grandjean texture and normal forces generated during shear. These effects can be explained in terms of the response of a correlated helical structure in the cholesteric mesophase to external stimuli. The shear induced transition associated with normal force generation is between the focal conic and homeotropic texture. In an effort to understand the responses of the cholesteric system to multiple stimuli, studies have been extended to include electric field effects.

This work reports on the effects of an electric field on the dynamic focal conic to homeotropic transition examined as a function of a transverse electric field applied under constant shearing conditions. It is shown that the field decreases the amount of shear required to produce the transition. Calculations based on the helical correlation model show that helical distortion must take place during field application. It is postulated that these distortions facilitate the focal conic to homeotropic transition. Application of the model allows calculation of an average molecular interaction dipole operable in the transition region.

1. Introduction

Recently we reported$^{(1,2)}$ shear induced texture changes in cholesteric liquid crystalline materials. These changes were associated with rheological changes from non-Newtonian to Newtonian; and from Newtonian to non-Newtonian behavior with increasing shear. The regions of distinct rheological behavior observed with increasing

---

†Presented in part at the Fourth International Liquid Crystal Conference, Kent State University, August 21–25, 1972.

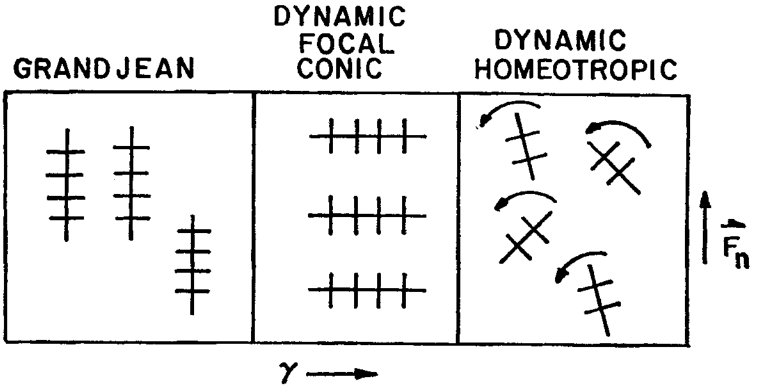

Figure 1. Schematic representation of the shear induced texture changes, based on the correlated helix model of Ref. 3.

shear were found to be associated with the Grandjean, focal conic and homeotropic textures respectively. The sheared mesophase in the Newtonian region has been shown⁽³⁾ to be comprised of a layered structure. The layers consist of perturbed and unperturbed Grandjean texture, and a highly scattering layer (called dynamic focal conic), believed to be comprised of helical correlations of molecules in which the helical axes are parallel to the shearing plane. One striking aspect of the studies was the observance of the shear induced focal conic to homeotropic transition accompanied by the appearance of appreciable normal forces. An interpretation of the data leads to a picture of the homeotropic mesophase as consisting of helical fragments (correlations of molecules in a helical array), whose lengths are less than the characteristic pitch length (P_0) of the unsheared material.⁽²⁾ The behavior according to the correlated helix model is illustrated schematically in Fig. 1. The dynamic homeotropic texture appears to involve tumbling of correlated rod-like molecular aggregates giving rise to the observed normal stresses.

The relation of normal stresses produced by the hydrodynamic interaction of rotating rod segments has been discussed by Kotaka.⁽⁴⁾ The primary normal stress difference, $P_{11}-P_{22}$, can be written in terms of the helical rod length, L (for sufficiently large aspect ratio), and the shear rate $\dot{\gamma}$ as:

$$P_{11}-P_{22}=\frac{K\dot{\gamma}^2 L^5}{[\ln(L/b)]^2} \tag{1}$$

where K contains the rod density and Newtonian viscosity terms in addition to numerical constants, and b is a characteristic spacing along the rod taken as 5 Å to correspond to the approximate molecular separation distance along the helical rod of length L. Calculations by iteration show that the dominant factor governing L is the shear rate at which normal stresses are observed (Fig. 2). L decreases with increasing shear rate from about 400 Å to about 200 Å and appears to approach a limiting value of less than 100 Å, if results are extrapolated to the high shear rate region. This is what would be expected as the rod segments, which are clusters of molecules, continue to be broken up by the increasing shear field. These values are less than 10% of the characteristic pitch values exhibited by the original cholesteric mixtures in the absence of shear. It has been reported that the static homeotropic texture which is thermally produced (and is unstable) is a medium of low anisotropy.$^{(5)}$ Sizes of molecular aggregates calculated from the normal stresses$^{(2)}$ and from

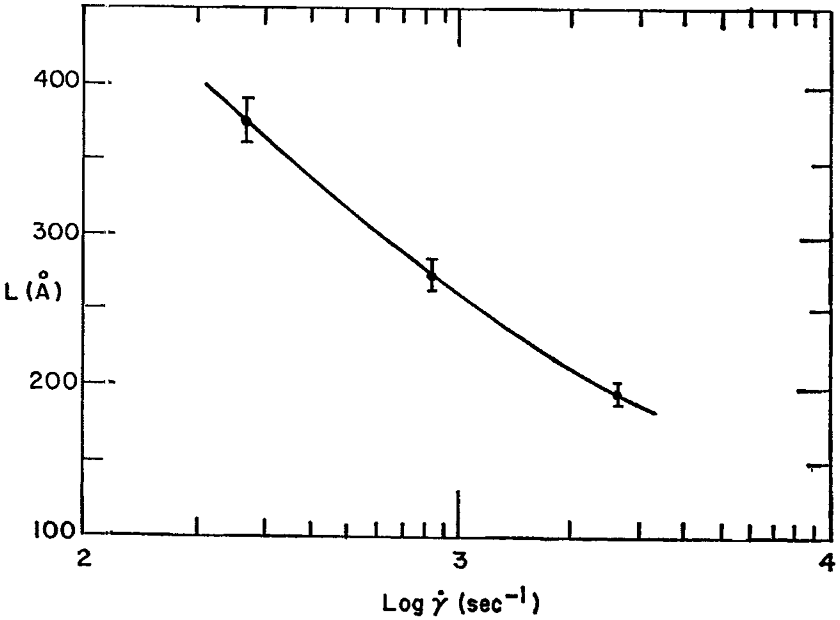

Figure 2. The shear rate dependence of helical fragment length L, in the homeotropic texture, calculated from the measured normal stress differences using Eq. (1). The error bars show the extent of variation with composition, as cited in Ref. 2.

light scattering⁽⁵⁾ appear to be in reasonable agreement, however.

One might expect that other external stimuli would affect the focal conic to homeotropic transition during shear. We now report the effect of electric field on the shear induced dynamic focal conic to homeotropic transition.

2. Experimental

The liquid crystal samples used were melt blended mixtures of cholesteryl-oleyl-carbonate (COC) (Eastman Kodak) and cholesteryl chloride (CCL) (Sigma Chemical Corporation). Both components were used without further purification but did exhibit melting points and mesophase–isotropic transitions within 2 °C of those reported in the literature. Care was taken during melt mixing so as not to overheat the samples and cause thermal decomposition. The compositions provided a broad temperature range of cholesteric mesophase including room temperature. Two compositions have been studied; 14 and 28 wt % CCL in COC. The pitch bands of the two materials were measured as ∼3600 Å and 6500 Å respectively. Neither of these samples exhibit significant temperature sensitivity of the pitch band. Similar systems have been studied optically in this laboratory.(6,7)

The Weissenberg Rheogoniometer, Model R18, was used for this study. In order that the shear induced transition could be observed, the cone and plate assembly was replaced with a pair of parallel glass plates. These plates were attached concentrically to the flat platens of the Weissenberg and held in place by adhesive. The glass plates were coated with a continuous thin layer of tin oxide. The device enabled continuous sample observation and application of a dc electric field during the application of shear. Care was taken to insure that the plates were not grounded and a potential was applied to the sample with a Kepco Model D.W.91 power supply using a sliding contact on the upper surface of the rotating plates (see Fig. 3). The experiments were conducted in short time duration to minimize the effect of viscous heating during the application of shear.(2)

3. Theory

The sheared cholesteric mesophase is proposed to consist of a central

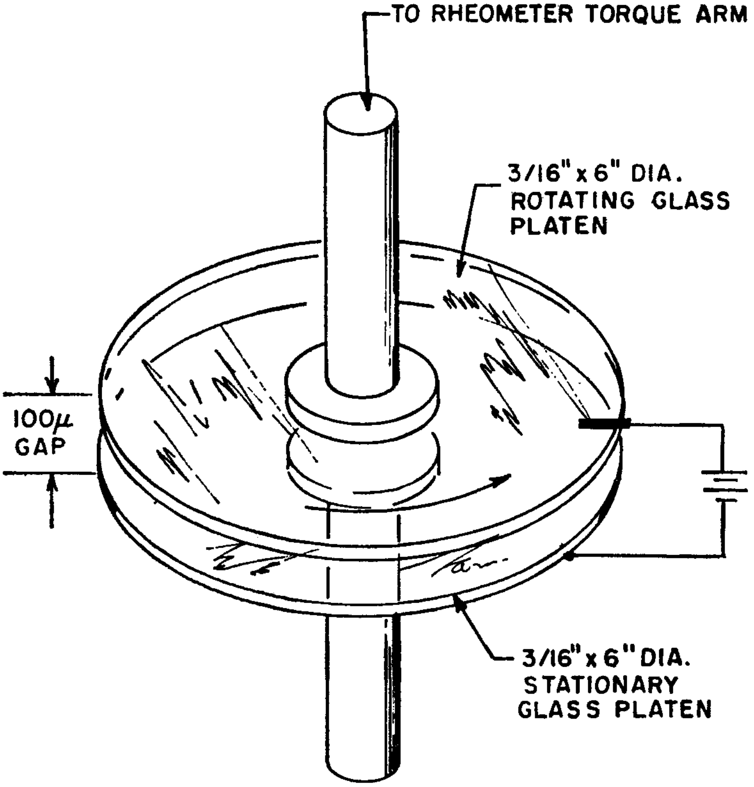

Figure 3. Glass platen configuration for the Weissenberg Rheogoniometer.

dynamic focal conic region interposed between layers of perturbed Grandjean texture.$^{(3)}$ The central layer is considered to be composed of time averaged helical correlations of molecules with the helical axes parallel to the shear field. The surrounding layers consist of tilted and untilted cholesteric helices normal to the surfaces. Consider now, a vector model of the dipole moment, μ, of a single cholesteric molecule. The molecule is considered to be an ellipsoid with the three principal axes as shown in Fig. 5.

In the helical conformation μ_z corresponds to the helical axis. A question arises as to the relative orientation of μ_z of the individual molecules: do they align parallel or anti-parallel in the helix conformation? If alignment were parallel the individual correlated

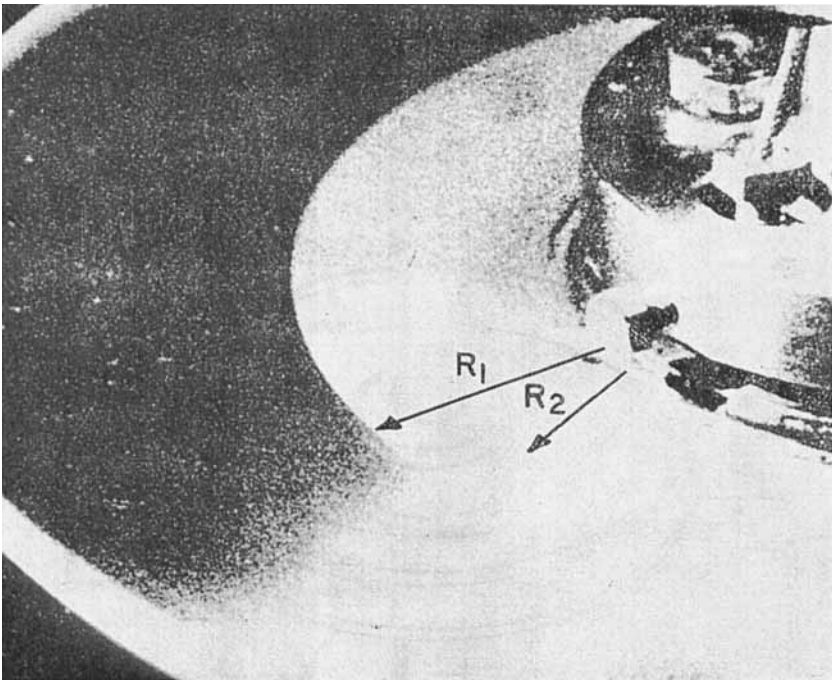

Figure 4. Photograph showing the shear induced focal-conic (inner area) to homeotropic (outer area) transition. Note the sharp boundary.

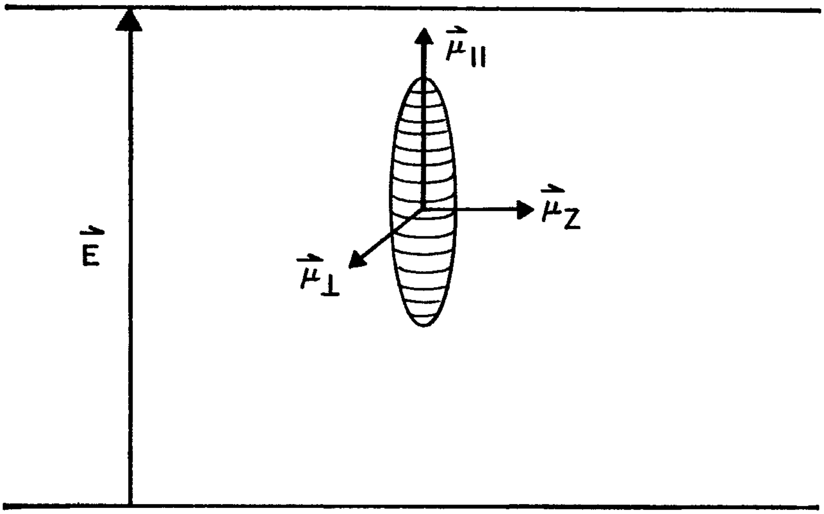

Figure 5. Schematic representing molecular dipole-field interactions.

helices would have very large dipoles equal to $n\boldsymbol{\mu}_z$ where n is the number of molecules correlated in a helix. There appears to be no experimental evidence for this. With an electric field (**E**) applied between the two electrodes (Fig. 3), the interaction energy of a cholesteric molecule in the electric field will be

$$E_n = -\boldsymbol{\mu}\cdot\mathbf{E} = -\boldsymbol{\mu}_{\parallel}\cdot\mathbf{E} - \boldsymbol{\mu}_z\cdot\mathbf{E} - \boldsymbol{\mu}_{\perp}\cdot\mathbf{E} \tag{2}$$

Consider now the effect of a transverse electric field on the dynamic focal conic texture.

If the helical axis of the mesophase is always aligned parallel to the electrode surfaces, then

$$-\boldsymbol{\mu}_z\cdot\mathbf{E} = -|\boldsymbol{\mu}_z||\mathbf{E}|\cos\theta = -|\boldsymbol{\mu}_z||\mathbf{E}|\cos 90^\circ = 0$$

and only $\boldsymbol{\mu}_{\perp}$ and $\boldsymbol{\mu}_{\parallel}$ can interact with the field. The dipolar interaction now becomes

$$E_n = -|\boldsymbol{\mu}_{\perp}||\mathbf{E}|\cos\theta - |\boldsymbol{\mu}_{\parallel}||\mathbf{E}|\cos\theta' \tag{3}$$

where θ and θ' are the angles that any given set of $\boldsymbol{\mu}_{\perp}$ and $\boldsymbol{\mu}_{\parallel}$ make with the applied field. Because of the helical correlation, each molecule will have a slightly different angular displacement from the one preceding it in the helix and thus, the energy of interaction must be averaged over all values of θ. The individual dipole orientations can be any value from 0° to 360°. It is seen from Eq. (3) that, if the helix is not distorted, averaging the two dipoles ($\boldsymbol{\mu}_{\parallel}$ and $\boldsymbol{\mu}_{\perp}$) over the 360° orientations of the helix will produce an average zero total interaction energy. At low fields where $\boldsymbol{\mu}\cdot\mathbf{E}$ is much less than the molecular correlation energy E_c of the helix, the applied potential should have little or no effect on the focal conic to homeotropic transition. At intermediate ($\boldsymbol{\mu}\cdot\mathbf{E} \sim E_c$) and high fields ($\boldsymbol{\mu}\cdot\mathbf{E} \gg E_c$) dipole alignment of the molecules with the applied field will occur. In the intermediate case this may result in a distorted helix, while in the high field case a cholesteric to nematic transition has been shown to proceed from Grandjean through focal conic texture with increasing field.(8) It is, thus, apparent that field distortion of the helical correlations causing a net dipole alignment with the applied field might first take place and that field dipole interactions can be expected to affect the rheologically induced transitions.

It is apparent from Fig. 4 that a critical shear ($\dot{\gamma}_c$) is needed for the shear induced transition. In the absence of an applied electric field this critical shear rate has been shown⁽²⁾ to be about $1.1 \times 10^3 \mathrm{sec}^{-1}$. The same value of $\dot{\gamma}_c$ has been observed from shearing between the tin oxide surface, as had been previously observed from glass surfaces.⁽²⁾ Application of an electric field shifts the transition boundary toward the rotation axis of the platens. With the field on, the applied shear rate could be lowered well below $10^3 \mathrm{sec}^{-1}$ and the focal conic–homeotropic boundary was still observed. Thus, application of the field decreases the stability of the sheared cholesteric state permitting the shear induced transition to take place at a lower shear rate, $\dot{\gamma}_{ce}$. The change in energy of the liquid crystal state (caused by the field application) (E_E), can be equated to the changes in shear energy required to produce the transition.

Thus,

$$E_E = \int_{R_1}^{R_2} \eta \frac{\omega}{l}\, \mathrm{d}r = \eta \frac{\omega}{l}(R_2 - R_1) = \eta \frac{\omega}{l} R_2 - C \tag{4}$$

where η is the Newtonian macroscopic viscosity⁽²⁾ of the dynamic focal conic state, ω is the angular speed of the platens, l the sample thickness, and R the measured radius at the transition boundary. (1 and 2 denoting before and after field application.) The term involving R_1, is a constant for a given angular speed, therefore Eq. (3) can be written:

$$\eta \frac{\omega}{l} R_2 = E_E + C \tag{5}$$

E_E involves induced dipole–field or dipole–field interactions and is the difference in interaction energy of the dipoles in the dynamic focal conic state and the homeotropic state. Since the homeotropic state is considered to have random orientations (a condition which should result to a first approximation in zero interaction energy) the field interactions in the dynamic focal conic state need only be considered. Usually dipole-field interactions are larger,⁽⁹⁾ and E_E would be expected to arise from dipole–field interactions in the helices. The energy balance can be written in terms of the orientation function $F(\theta, \phi)$ of the distorted system as:

$$E_E = \int_0^{2\pi} \int_0^{\pi} n \,|\boldsymbol{\mu}|\,|\mathbf{E}|\, F(\theta, \phi) \cos\theta d\, \theta d\phi \tag{6}$$

where n is number density of dipoles, and $F(\theta, \phi)$ the angular distribution of dipoles. For a one component system n and $|\boldsymbol{\mu}|$ are constant. For a constant DC field, Eq. (6) can be written:

$$E_E = n || \boldsymbol{\mu} | \mathbf{E} | \int_0^{2\pi}\int_0^{\pi} F(\theta, \phi) \cos\theta d\theta d\phi = n | \mathbf{E} | \langle \mu \rangle \tag{7}$$

where $\langle\mu\rangle$ represents the distribution averaged dipole interacting with the applied electric field; $(\langle\mu\rangle = |\boldsymbol{\mu}| \langle F(\theta,\phi)\rangle)$. $F(\theta,\phi)$ would be expected to encompass Boltzmann averaging of all orientations of the dipole in the helices under shearing conditions. Since we have no way of ascertaining the helical configuration during shearing, the integral containing the distribution function is not evaluated and is written as $\langle F(\theta,\phi)\rangle$, indicating the integration and averaging of the dipole orientation over the angles θ and ϕ.(10)

For a two component system, two dipoles $\boldsymbol{\mu}_1$ and $\boldsymbol{\mu}_2$ are operative. However, since the two component system exhibits a single pitch,(3) $F(\theta,\phi)$ would describe the orientation of either moment (a continuous function over the helix) and Eq. (6) should be written:

$$E_E = \int_0^{2\pi}\int_0^{\pi} \Sigma_i n_i | \boldsymbol{\mu}_i | \mathbf{E} | F(\theta, \phi) \cos\theta d\theta d\phi \tag{8}$$

Eq. (5) is then:

$$\dot{\gamma}_{ce} \frac{\omega}{l} R_2 = \frac{n | \mathbf{E} |}{\eta} \langle \mu \rangle + C$$

where $\langle\bar{\mu}\rangle$ is the averaged interaction dipole adjusted for composition. A plot of $\dot{\gamma}_{ce}$ vs. $|\mathbf{E}|$ might be expected to produce insight into the changes in Boltzmann's averaged orientation function with field. If the plot is linear, an average interaction dipole can be calculated.

4. Results and Discussion

Figures 6 and 7 contain plots of $\dot{\gamma}_{ce}$ versus applied electric field (volts/micron) for two mixtures of COC/CCL. As seen in Fig. 6 two regions are observed in the plot; a low field region in which the transition is not affected to any great extent by electric field, and a higher field region in which $\dot{\gamma}_{ce}$ is a linear function of $|\mathbf{E}|$. Both field regions were only observed in the sample containing 28% CCL. However, it is apparent from the single measured point at low field in the 14% CCL sample (Fig. 7) that this mixture would exhibit similar behavior. We also note that the effects observed as a function

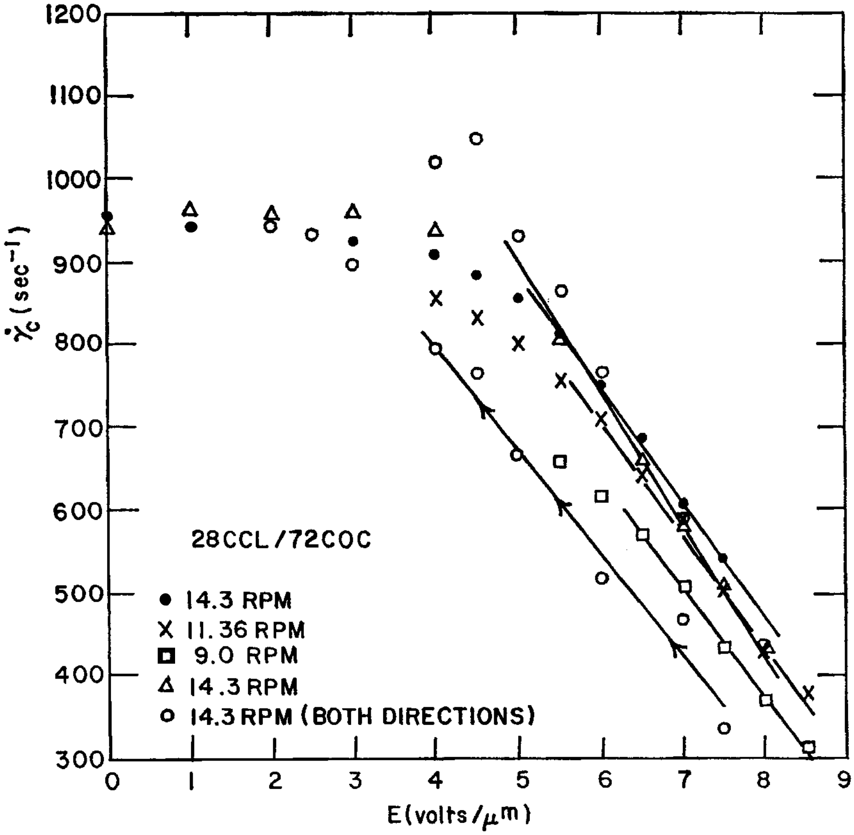

Figure 6. Critical shear rate ($\dot{\gamma}_{ce}$) vs. applied field | E | for the focal-conic to homeotropic transition in a 28% CCL mixture in COC.

of electric field occur, for the most part, below 8 V/μ. For the mixtures used in these experiments this is far below the threshold voltage of the cholesteric–nematic phase transition. A nearly compensated mixture of CCL/COC (50/50) [$P_0 \gg 2.0\mu$] has been studied and exhibited a threshold voltage of 8 V/μ. As the threshold voltage has already been shown to be proportional to the inverse pitch,(8) the threshold voltage for the mixtures used in this study would be expected to be much higher than 8 V/μ, therefore the transition observed would not be due to the field induced cholesteric–nematic phase transitions.

Movement of the transition boundary with a change in field was

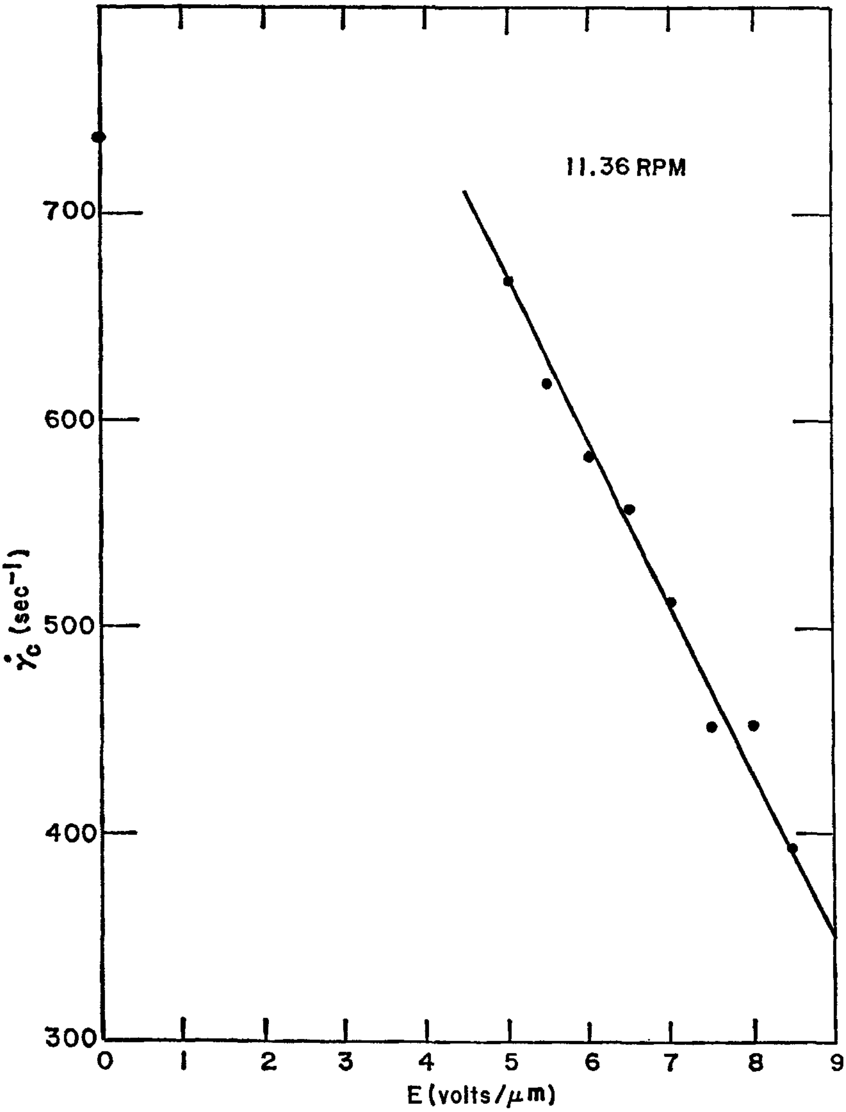

Figure 7. Critical shear rate ($\dot{\gamma}_{ce}$) vs. applied field $|\mathbf{E}|$ for the focal-conic to homeotropic transition in a 14% CCL mixture in COC.

found to be time dependent and not instantaneous. Upon application of a sufficient field to perturb the boundary, an area of turbulence and transformation occurred in the region that would eventually

TABLE 1 Slope of $\dot{\gamma}_{ce}$ vs. $|\mathbf{E}|$ in high field linear portions for CCL/COC mixtures[a]

Sample	Experimental run	Slope[b]	μ[c]
14% CCL/86% COC	1	79	0.087
28% CCL/72% COC	1	140	0.167
28% CCL/72% COC	2	137	0.164
28% CCL/72% COC	3	135	0.161
28% CCL/72% COC	4	124	0.148
28% CCL/72% COC	5	155	0.185

[a] All samples were measured at 100μ thickness.

[b] Standard least squares analysis. (sec^{-1} volt^{-1} μ)

[c] Calculated using a density of 1 gm/cc. (esu-cm × 10^{18})

transform and after a period of approximately 5 to 10 sec the new transition boundary would form and stabilize. Upon removal of the field the reverse would happen although more rapidly. Fig. 6 shows variation in $\dot{\gamma}_{ce}$ with various experimental runs and platen rotation velocities. The high field linear regions of the figure show some day to day variation but their slopes are very similar. This data is seen in Table 1 in which the slope of the various $\dot{\gamma}_{ce} - |\mathbf{E}|$ curves (in the high field linear region) are presented. $\langle\mu\rangle$ from Eq. (9) using $\eta_0 = 40$ poise (the measured value of the focal conic viscosity)(2) is shown in the table.

The $\langle\mu\rangle$ calculated for all samples are approximately 0.15 debye. This value fits the description of the transition quite well. In the dynamic focal conic texture the dipolar interaction energy was shown to be zero at low fields. At intermediate fields the helices probably distort, permitting a net dipolar interaction. Since the helical distortion could be quite complicated, there is no way of ascertaining $F(\theta,\phi)$.

The calculated values of $\langle\mu\rangle$ are reasonable. The linearity of the $\dot{\gamma}_{ce}$ vs. $|\mathbf{E}|$ plots shows the molecular structure to be such that an almost constant dipolar interaction takes place with the applied field after a significant field has been attained. The constancy of the dipolar interaction indicates that after a threshold value of field has been attained $|\boldsymbol{\mu}|\,\langle F(\theta,\phi)\rangle$ is constant and, therefore, $F(\theta,\phi)$ is constant. This would imply that the cholesteric helix will only distort a finite amount before disruption of long range correlation occurs producing the dynamic homeotropic texture. The finite amount of energy expended to distort the helix must be equal to the disruption energy for the helix under the shearing conditions. There is no way at present of ascertaining whether this distortion persists in the homeotropic texture.

It appears that increasing the amount of CCL in the mixture results in an increase in μ. This could mean that the dipole moment of CCL is larger than that of COC and thus increases the field interaction of the helix.

The sheared state prior to transformation is known to be a layered structure.(3) Changing the effective sample thickness may involve increasing the field interaction with the helices stabilized by the platen surface. The proportion of immobilized surface to volume would increase and might possibly require the higher fields for the 14% CCL sample. Surface interactions may also stabilize the transformed state and not permit total relaxation at the cessation of field application.

The fields required in the mixed systems may be due to the larger pitch of the cholesteric mixture. COC forms a left-handed helix with $P_0 \sim 3420$ Å, while CCL is right-handed with a pitch of 4880 Å. Mixtures have pitches larger than either pure component, and since the critical field E_{TH} for cholesteric to nematic transitions is known to be an inverse function of pitch,(8) field disruption of the dynamic focal conic texture might also be more facile with a higher pitched material.

In conclusion, we have shown that the shear induced dynamic focal conic to homeotropic texture can be changed by the application of an electric field. The effect is associated with distortion of the cholesteric helical structure permitting partial alignment of molecular dipole moments within the helix. It appears that a critically distorted structure which is dynamically unstable results and undergoes a transition to the homeotropic texture. Average interaction dipoles causing the transitions have been calculated and appear reasonable.

REFERENCES

1. Pochan, J. M. and Erhardt, P. F., *Phys. Rev. Letters* **27**, 740 (1971).
2. Erhardt, P. F., Pochan, J. M. and Richards, W. C., *J. Chem. Phys.* **57**, 3596 (1972).
3. Pochan, J. M. and Marsh, D. G., *J. Chem. Phys.* **51**, 1193 (1972).

4. Kotaka, T., *J. Chem. Phys.* **30**, 1566 (1959).
5. Asada, T. and Stein, R. S., Fourth International Liquid Crystal Conference, Kent State University, August 1972.
6. Adams, J., Haas, W. and Wysocki, J., *Phys. Rev. Letters* **22**, 92 (1969).
7. Adams, J., Haas. W. and Wysocki, J., *J. Chem. Phys.* **50**, 2458 (1969).
8. Wysocki, J. J., Adams, J. F. and Olechna, D. J., *Liquid Crystals and Ordered Fluids*, J. F. Johnson and R. S. Porter, eds., Plenum Press, New York, New York, 1970, p. 419.
9. Wollrab, J. E., *Rotational Spectra and Molecular Structure*, Academic Press, New York, New York, 1967, p. 262.
10. Davidson, N., *Statistical Mechanics*, McGraw-Hill Book Co., New York, New York, 1962.